Crystal Structure Analysis of CuCro$_2$ Based On XRD Data Using GSAS Software

Lalu A. Didik[1], Muh. Wahyudi[2]

[1]Departement of Physics Education, Faculty of Tarbiya and Education, Universitas Islam Negeri Mataram. Email: laludidik@uinmataram.ac.id

[2]Departement of Physics Education, Faculty of Tarbiya and Education, Universitas Islam Negeri Mataram. Email: muh.wahyudi@uinmataram.ac.id

ABSTRACT

The synthesis of CuCrO$_2$ crystals by mixing CuO and Cr$_2$O$_3$ has been carried out using the solid reaction method at a temperature of 1200 ^{0}C. The characterization of the structure used XRD and analyzed using GSAS software. The results of characterization using XRD showed that no other phase occurred. This is evidenced by the absence of other phases from the results of refinement of measurement data with reference data and a value of χ 2 which is 1.222. The lattice parameter values resulting from the refinement of the CuCrO2 X-ray diffraction pattern are a = b = 2.9715 Å and c = 17.1104 Å with a cell volume of 130.584 Å 3. In addition to the lattice parameter values, the distance between atoms was also obtained, both Cu - O, Cr - Cr, and Cr - O.

Introduction

In recent years, antiferromagnetic materials have become the subject of relatively large studies in material physics. Lattice systems and geometric structures in two dimensions (2D) have become a concern. One of the interesting studies is delafossite compounds [1–9].

CuCrO$_2$ is a very interesting focus for p-type of TCO. This compound is transparent to visible light even though there is a forbidden 3d dipole centered on Cr in the visible region. CuCrO$_2$ has a measured hole mobility of 11 cm²/Vs with a charge carrier concentration of about 4,75 x 10^{17} cm^{-3} in the dopant impurity [10].

CuCrO$_2$ structure in the space group number 169 at room temperature (in hexagonal form with lattice parameters a = 2.976 A and c = 17.1104 A at room temperature). Only the octahedron of CrO$_6$ has T$_N$ = 24 K and shows short magnetic correlations along the c axis. The maximum magnetic moment of CuCrO$_2$ is around 3 μB [11,12].

Analyze the structure of a crystal in general using X-Ray Diffraction (XRD). XRD analysis result data is matched with a database, one of which is ICDD (International Center for Diffraction Data). However, the use of ICDD is still very limited to phase matching and analysis of the atomic position of the composition of crystals, but it has not been able to analyze other crystal structure parameters such as lattice parameters, bond lengths between crystal atoms and volume. Therefore, we need crystal structure software analyze such as Rietica, PCW and GSAS (General Structure Analysis System).

The software that can analyze the complete crystal structure both lattice parameters and bond lengths between atoms is GSAS. GSAS is a software that can simultaneously analyze all the data generated by X-ray diffraction and neutron diffraction [13,14]. The GSAS method refers to the refinement method based on Rietveld analysis. This analysis refers to the refinement of the structure by matching the overall X-ray diffraction pattern to obtain microstructure data more accurate [15].

Several studies have used GSAS software to analyze the structure of a crystal [13,14]. However, no one has analyzed the structure of $CuCrO_2$ and the bond lengths between its atoms that synthesized by solid state reaction method used GSAS. Therefore, in this study, analysis of $CuCrO_2$ structure (refinement data, lattice parameters and spacing between constituent atoms) was carried out using GSAS software.

Experimental Method

$CuCrO_2$ crystals were synthesized through a solid reaction method of the preparation oxide CuO (Physical Analysis 99% from Sigma Aldriech) and Cr_2O_3 (Physical Analysis 99% from Sigma Aldriech) mixed with a stoichiometric ratio of 2 : 1 [7,16]. The material is then crushed for 4 hours using a mortar to make it homogeneous and to obtain a relatively small particle size [13,17]. With a relatively small particle size, it is expected that it will facilitate diffusion between particles during sintering so that $CuCrO_2$ crystals will form in a single phase according to equation 1.

$$2CuO + Cr_2O_3 \rightarrow 2CuCrO_2 + \frac{1}{2} O_2 \qquad (1)$$
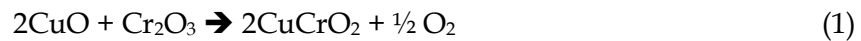
The sample is then compacted in a mold with a pressure of 200 bar so that it forms a pellet with a diameter of 1 cm. Samples were heated in a furnace at a temperature of 1200 ^{0}C with an increase in temperature of 1 ^{0}C per minute and held for 12 hours [16]. The analysis of the crystal structure in the sample using the Philip PW1710 X-ray Diffraction. The measurement of the diffraction pattern of the sample was carried out with an X-ray beam from a Cu Kα anode tube with a wavelength of λ = 1.5406 Å in a continuous step mode.

Table 1. Position of $CuCrO_2$ constituent atoms to obtain reference XRD patterns

Atomic Position	x	y	z	Occupation
Cu	0	0	0	1
Cr	1/2	1/2	1/2	1
O	1/9	1/9	1/9	2

The reference diffraction pattern data is obtained from the $CuCrO_2$ wick off table data with space group number 169 and the atomic positions shown in Table 1. The reference structure of R-3m is in hexagonal form with lattice parameters a = 2.976 Å and c = 17.1104 Å. This reference data is obtained from the American Mineralogy Crystal Structure Database. The sample XRD measurement results data then refinement with a reference diffraction pattern using GSAS software to obtain lattice parameter data and the distance between sample atoms.

Result and Discussion

GSAS software was used to determine the crystallography of the sample. The resulting crystallographic data are in the form of lattice parameters and the distance between atoms based on the principle of refinement of the sample X-ray diffraction data combined with the reference X-ray data as shown in Figure 1.
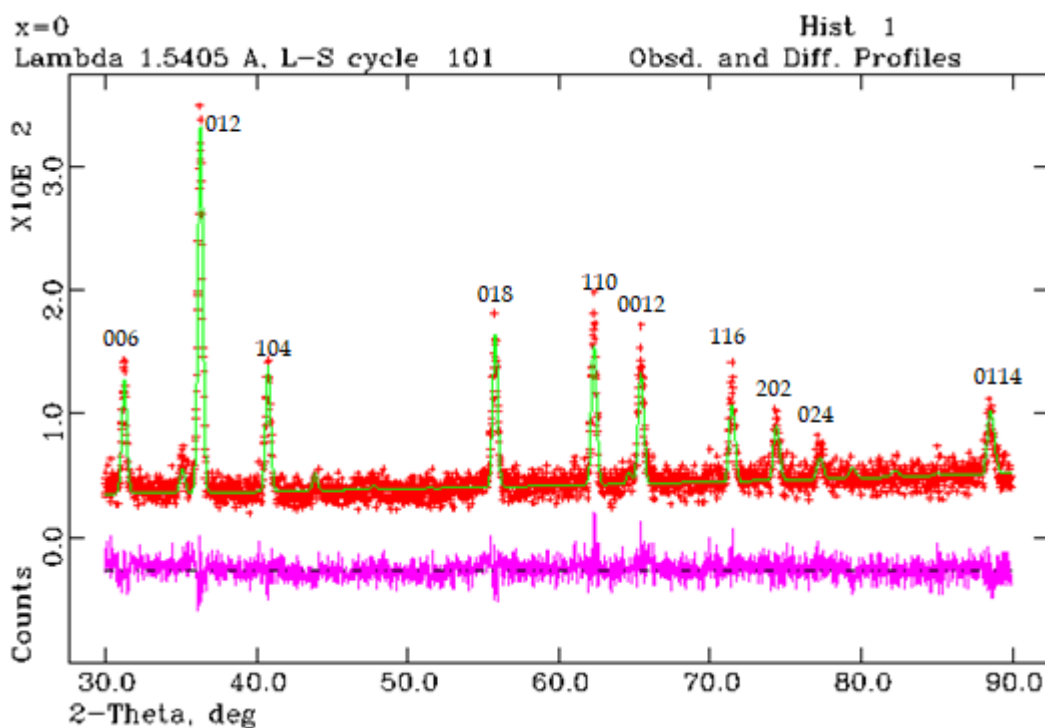

Figure 1. Refinement Curve between The Observation Curve and The Calculation Curve by Means GSAS

Figure 1 shows that the refinement curve between the observation curve (measured using XRD) and the calculation curve (the calculated curve using the reference) looks almost coincided. The red curve shows the crystal intensity of the XRD results, while the green curve shows the intensity of the reference analyze. The difference between the two curves which indicates that the curve from the normalized error distribution only leaves the background peaks from the sample measurements (purple curve). The quality of the fittings is also showing a very good level. This is indicated by the value of χ of 1.222 which is close to the value of 1 and the value of Rp which is only 12.65%. The value of χ shows the level of

truth of the experiment. If the χ value is close to 1, the research will be close to ideal. The value of χ is still within the limit because the maximum value allowed is 1.3 [14].

Each of the atoms in the crystal will reflect the X-rays that are dropped on crystals in all directions, but only in one particular direction the reflected waves will make constructive interference. Suppose that the sequence of atoms in the crystal is d each other, then each of these fields on the atom will reflect part of the beam X-rays that are dropped on the crystal. The wave front reflected by the second plane will left behind that reflected by the leading plane because the waves reflected by the second plane will have distance additional 2 d sin θ where θ is the angle of rays measured from the surface of the crystal. If the difference is equal to an integer multiple of the wavelength, the beams are reflected by interfere constructively so as to provide and the intensity will be maximum. This theory is known as Braggs Law. Thus, a fundamental statement for maximum interference in X-ray diffraction in the crystal is indicated by equation 1 [15].

$$2 \text{ d} \sin \theta = n\lambda \qquad n = 1, 2, 3, ……$$ (1)

The X-ray diffraction pattern of the model with the diffraction pattern of the sample fits without any other phase. The diffraction pattern of $CuCrO_2$ with a distinctive peak at each 2 theta angle indicates that the resulting sample is a single phase of polycrystalline $CuCrO_2$. The diffraction peaks produced in this study have a small widening pattern, which indicates a large sample crystal size. This means that the width of the diffraction peak provides information about the size of the crystal [18].

The large crystals have a large area of X-ray reflection. The diffraction peaks are generated by constructive interference of rays reflected by the crystal planes. In the theory of wave interference, the greater the number of interference gaps, the narrower the fringe size on the screen. Multiple slit interference with an infinite number of slits produces a small, but very bright, number of fringes. That is why large crystal sizes tend to have a narrow peak width. The crystal structure data of the refinement results are shown in Table 2.

Table 2. Crystallographic data and lattice parameters from Refinement of measurement data and reference data for $CuCrO_2$ crystals

Crystal System	Rombohedral		
Space Group	R-3m (169)		
Parameters	a (Å)	b (Å)	c (Å)
	2,9715	2,9715	17,0765
Standard Deviation	0,0004	0,004	0,0027
	A	B	Γ
	90^0	90^0	120^0
Cell volume (Å³)	130,584		
Crystal Size (nm)	132		
χ^2	1,222		
wRp	16,1 %		
Rp	12,65 %		

The value of the $CuCrO_2$ crystal lattice parameter obtained using the X-ray diffraction method has the same value as the crystal lattice parameter measurement using other methods such as the neutron diffraction method. This is because both the X-ray diffraction

method and the neutron diffraction method have the same measurement principle, namely the Rietveld method. The comparison of $CuCrO_2$ lattice parameters measurements with X-ray diffraction and neutron diffraction methods is shown in Table 3.

Table 3. Comparison of the results of measurements of $CuCrO_2$ lattice parameters with different methods

Method Measurement	Parameters		χ^2	Cell Volume ($\mathring{A}^3$)	Reference
	a = b ($\mathring{A}$)	c ($\mathring{A}$)			
X Ray Diffraction	2,9715	17,0765	1,222	130,584	This Research
Neutron Diffraction	2,9760	17,1104	2,97	131,2	[1]

Table 4 shows the distance between the atoms of $CuCrO_2$ from the refinement of the XRD diffraction pattern of the sample. The distance between atoms is very useful if we want to know the physical properties of $CuCrO_2$ crystals, for example to determine the effect of doping other ions on the physical properties of $CuCrO_2$ crystals.

Table 4. The Distance Between Atomic Composer $CuCrO_2$ Results of Refinement Using GSAS Software

Vector	Distance Between Atom ($\mathring{A}$)	Field Index	Nearest Atomic Coordinates		
			x	y	z
Cu – O	1,897	1 0 0	0	0	0,111
Cu - O	1,897	-1 0 0	0	0	-0,111
Cr – Cr	2,971	1 -1 -1	-1	-1	0,5
Cr – Cr	2,971	1 -1 0	-1	0	0,5
Cr – Cr	2,971	1 0 -1	0	-1	0,5
Cr – Cr	2,971	1 0 1	0	1	0,5
Cr – Cr	2,971	1 1 0	1	0	0,5
Cr – Cr	2,971	1 1 1	1	1	0,5
Cr – O	1,960	-101 -1 -1	-0,6667	-0,3333	0,5557
Cr – O	1,960	-101 0 -1	0,3333	-0,3333	0,5557
Cr – O	1,960	-101 0 0	0,3333	0,6667	0,5557
Cr – O	1,960	-201 -1 -1	-0,3333	-0,6667	0,4447
Cr – O	1,969	-201 0 -1	-0,3333	0,3333	0,4447
Cr – O	1,960	-201 -1 -1	0,6667	0,3333	0,4447

Figure 2 shows the crystal structure of $CuCrO_2$. It appears that there are 2 important elements, namely Cu-O dumbbells and CrO_6 layers where each element affects the physical properties of $CuCrO_2$ crystals. The electrical properties of $CuCrO_2$ are influenced by Cu-O dumbbells [19], [20] while the magnetic properties are influenced by the planar CrO_6 [12,21]. If the distance between Cu - O gets bigger, the atomic volume will be bigger which will make the electrons along the dumbbell move easier so that it will increase the conductivity value [16,22].
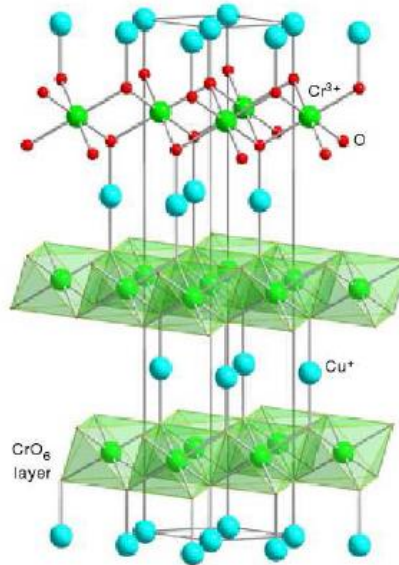
Figure 2. Crystal Structure CuCrO2 [12]

Magnetic properties are influenced by the bond length between Cr and O atoms. Each Cr ion is surrounded by 6 closest neighbors and 6 next closest neighbors [23]. Only the octahedran portion of CrO_6 shows a short magnetic correlation along the c axis [11,12].

Conclusion

The synthesis of single $CuCrO_2$ has been successfully carried out using the solid reaction method. The results of characterization using XRD showed that no other phase occurred. This is evidenced by the absence of other phases from the results of the refinement of measurement data with reference data and the value of χ which is still within the normal limit, namely 1.222. The lattice parameter values resulting from the refinement of the $CuCrO_2$ X-ray diffraction pattern are a = b = 2.9715 Å and c = 17.1104 Å with a cell volume of 130.584 Å ^{3}. In addition to the lattice parameter values, the distance between atoms was also obtained, both Cu - O, Cr - Cr, and Cr - O.

References

[1]   M. Poienar, F. Damay, C. Martin, V. Hardy, A. Maignan, and G. André, (2009). Structural and magnetic properties of $CuCr_{1-x}Mg_xO_2$ by neutron powder diffraction, *Phys. Rev. B - Condens. Matter Mater. Phys.*, 79 (1), pp. 1–8, doi: 10.1103/PhysRevB.79.014412.

[2]   M. Amami, S. Smari, K. Tayeb, P. Strobel, and A. Ben Salah, (2011). Cationic doping effect on the structural , magnetic and spectroscopic properties of delafossite oxides $CuCr_{1-x}(Sc,Mg)_xO_2$, *Mater. Chem. Phys.*, 128 (1–2), pp. 298–302, doi: 10.1016/j.matchemphys.2011.03.021.

[3]   A. T. Apostolov, I. N. Apostolova, and J. M. Wesselinowa, (2019). Ferroelectricity in the multiferroic delafossite $CuFeO_2$ induced by ion doping or magnetic field, *Solid State Commun.*, 292, pp. 11–16, 2019, doi: 10.1016/j.ssc.2019.01.014.

[4]   C. F. O, S. Pantian, R. Sakdanuphab, and A. Sakulkalavek, (2017). Effect of starch addition on structural , electrical and thermal properties of Delafossite, *Materials Science & Engineering B*, 226, pp. 39–46, doi: 10.1016/j.mseb.2017.08.029.

[5]   H. Chen and J. Fu, (2014). Delafossite – $CuFeO_2$ thin films prepared by atmospheric pressure plasma annealing, *Mater. Lett.*, 120, pp. 47–49, doi: 10.1016/j.matlet.2014.01.017.

[6]   A. Barnabé, E. Mugnier, L. Presmanes, and P. Tailhades, (2006). Preparation of delafossite $CuFeO_2$ thin films by rf-sputtering on conventional glass substrate, *Mater. Lett.*, 60, pp. 3468–3470, doi: 10.1016/j.matlet.2006.03.033.

[7]   E. Guilmeau *et al.*, (2018). Mg substitution in $CuCrO_2$ delafossite compounds, *Solid State Communications*, 151, pp. 1798–1801, doi: 10.1016/j.ssc.2011.08.023.

[8]   C. T. Crespo, (2018). Potentiality of $CuFeO_2$-delafossite as a solar energy converter, *Sol. Energy*, 163, pp. 162–166, doi: 10.1016/j.solener.2018.01.091.

[9]   J. Ahmed and Y. Mao, (2016). Characterization and electrocatalytic properties of $CuGaO_2$, *J. Solid State Chem.*, 242, pp. 77–85, doi: 10.1016/j.jssc.2016.07.006.

[10]   Arnold, T., Payne, D. J., Bourlange, A., Hu, J. P., Egdell, R. G., Piper, L. F. J., Watson, (2009). X-ray Spectroscopic Study of The Electronic Structure of $CuCrO_2$, *Phys. Rev. B*, 79 (7), doi: doi:10.1103/physrevb.79.075102.

[11]   M. Kumar and C. Persson, (2013). Structural , electronic and optical properties of silver delafossite oxides : A first-principles study with hybrid functional, *Phys. B Phys. Condens. Matter*, 422, pp. 20–27, doi: 10.1016/j.physb.2013.04.035.

[12]   A. Maignan Martin, C., Frésard, R., Eyert, V., Guilmeau, E., Hébert, S., Poienar, M. Pelloquin, D., (2009). On the strong impact of doping in the triangular antiferromagnet $CuCrO_2$, *Solid State Commun.*, 149 (23–24), pp. 962–967, 2009, doi: 10.1016/j.ssc.2009.02.026.

[13]   W. A. Sebayang, P., Muljadi., Adi, (2010). Analisis Struktur Kristal $SrO_6Fe_2O_3$ Menggunakan Program General Structure Analysis System dan Pengujian Sifat Magnetnya., *J. Sains Mater. Indones.*, 12, pp. 215-220.

[14]   S. D. Yudanto and Y. Yuswono, (2018). Analisis Struktur dan Permodelan Kristal Calcium Manganese Oxide ($CaMnO_3$), *Metalurgi*, 29 (1), 27-32, 2018, doi: 10.14203/metalurgi.v29i1.268.

[15]   L. A. Didik, (2020). Penentuan Ukuran Butir Kristal $CuCr_{0,98}Ni_{0,02}O_2$ dengan Menggunakan X-Ray Difraction (XRD) dan Scanning Electron Microscope (SEM), *Indones. Phys. Rev.*, 3 (1), pp. 6–14, doi: https://doi.org/10.29303/ip r.v3i1.37.

[16]   T. N. M. Ngo, U. Adem, and T. T. M. Palstra, (2017). The origin of thermally stimulated depolarization currents in multiferroic, *Appl. Phys. Lett.*, 106, pp. 152904, doi: 10.1063/1.4918747.

[17]   L. A. Didik, (2016). Pengaruh Pemberian Medan Magnet Terhadap Konstanta Dielektrik Material $AgCrO_2$, *KONSTAN*, 2 (1), pp. 1–5.

[18] L. A. Didik, (2019). Analisa Efek Jahn Teller Terhadap Struktur Kristal Senyawa Delafossite $AgCr_{1-x}Ni_xO_2$ (0,01 ≤ x ≤ 0,04), *Indones. Phys. Rev.*, 2 (2), pp. 49–56, doi: https://doi.org/10.29303/i pr.v2v2.22.

[19] F. Jlaiel, M. Amami, N. Boudjada, P. Strobel, and A. Ben Salah, (2011). Metal transition doping effect on the structural and physical properties of delafossite-type oxide $CuCrO_2$, *J. Alloys Compd.*, 509 (29), pp. 7784–7788, doi: 10.1016/j.jallcom.2011.04.153.

[20] M. Asemi, M., & Ghanaatshoar, (2016). Conductivity Improvement of $CuCrO_2$ Nanoparticles by Zn Doping and their Application in Solid-State Dye-Sensitized Solar Cells, *Ceram. Int.*, 42 (6), pp. 6664–6672, doi: doi:10.1016/j.ceramint.2016.01.017.

[21] T. Elkhouni, M. Amami, C. V Colin, P. Strobel, and A. Ben Salah, (2013). Synthesis , Structural and Magnetic Studies of the $CuCr_{1-x}Co_xO_2$ Delafossite Oxide, *J. Magn. Magn. Mater.*, 330, pp. 101–105, doi: 10.1016/j.jmmm.2012.10.037.

[22] D. Xiong, Q. Zhang, S. Kumar, H. Li, and W. Chen, (2016). Use of delafossite oxides $CuCr_{1-x}Ga_xO_2$ nanocrystals in p-type dye-sensitized solar cell, *Journal of Alloys and Compounds*, 662, pp. 374–380, doi: 10.1016/j.jallcom.2015.12.044.

[23] F. Lin, C. Gao, X. Zhou, W. Shi, and A. Liu, (2013). Magnetic , electrical and optical properties of p-type Fe-doped $CuCrO_2$ semiconductor thin films, *J. Alloys Compd.*, 581, pp. 502–507, doi: 10.1016/j.jallcom.2013.07.160.